JOURNAL OF MATERIALS SCIENCE 24 (1989) 409–412

Study of the kinetics of decomposition of goethite *in vacuo* and pore structure of product particles

M. PELINO, L. TORO, M. PETRONI, A. FLORINDI, C. CANTALINI
Dipartimento di Chimica, Ingegneria, Chimica e Materiali, Universita de L'Aquila, 67040 Monteluco di Roio, L'Aquila, Italy

The kinetics of decomposition of α-goethite were investigated, under vacuum conditions, in the temperature range 170–250° C. The experimental thermogravimetric traces were interpreted according to the shrinking core model for cylindrical particles. The Arrhenius plot of ln$K$ (kinetic constant) against $1/T$ yielded an activation energy of 119 ± 9 kJ mol^{-1} at 210° C. The highest specific area, S_{BET} = 118.4 ± 5.5 m^2 g^{-1}, of the reaction product α-hematite, was obtained by decompsition at 225° C. Information about the formation of micropores and their evolution with temperature was also obtained.

1. Introduction

The decomposition reaction of α-goethite to yield α-hematite

$$2\alpha\text{-FeOOH (s)} = \alpha\text{-Fe}_2\text{O}_3\text{ (s)} + \text{H}_2\text{O (v)} \quad (1)$$

is a very important process in the production of catalytic materials, magnetic recording medium of γ-Fe$_2$O$_3$, colouring pigments and, more recently, humidity and gas ceramic sensors.

The decomposition behaviour of α-goethite has been extensively studied by means of different experimental techniques and in different atmospheres [1–8]. The products of the reaction were analysed by scanning and transmission electron microscopy [9–13], by X-ray diffraction [4, 6] and by adsorption measurements [7, 14–17].

The topotactic nature of the decomposition has been proposed by Van Oosterhout [11], and in a recent review details of the solid state reaction have been extensively discussed by Volpe and Boudart [18]. They pointed out the lack of quantitative and reproducible studies of the kinetics of reaction involving solids and the influence of experimental variables, such as particle dimension, bed dimension and heat transfer on the reaction regime.

This study was undertaken with the aim of obtaining the kinetics of decomposition of α-goethite powder, in a temperature range 170–250° C, by means of thermal and differential thermal analysis, TG and DTA. Information concerning the evolution of the structure, the formation of micropores and their modification as function of temperature were also obtained by nitrogen adsorption, scanning and transmission electron microscopy.

2. Experimental procedure

The acicular goethite samples used in this work were supplied by the Bayer Co. The purity of the sample was controlled by X-ray analysis.

The shape and the dimensions of the particles were determined by scanning electron microscopy, taking several pictures of the sample and comparing the particles with the reference marker. All the particles observed had a cylindrical shape as shown in Fig. 1a.

The dimensions of about 200 particles of α-goethite were determined in over 20 pictures and the obtained measurements were compiled in ranges differing by 0.05 μm. The average dimensions of the goethite particles were determined by evaluating the statistical weight of each range; the resulting values of the radius and the length were obtained as 0.10 ± 0.01 μm and 1.0 ± 0.1 μm respectively.

The specific area, measured by the BET method and employing a Carlo Erba liquid nitrogen Sorptomatic mod. 1800, was found to be 14.1 ± 0.3 m^2 g^{-1}, where the associated error is an overall evaluation of the errors asociated with the BET method.

The experimental runs of decomposition of α-goethite were carried out as described below.

About 100 mg of the sample was heated in a stainless steel boat, suspended from the left arm of a computerized Cahn 1000 microbalance, in an evacuated quartz apparatus. The boat was immersed in an oil bath with electronic thermostat, previously heated to the desired temperature. The decomposition of acicular goethite was carried out at 170, 180, 190, 200, 225 and 250° C. The experimental temperature was assumed to be the same as that of the oil and controlled by a calibrated thermometer. The vacuum in the apparatus was maintained below 1×10^{-5} torr in all runs by means of diffusion and mechanical pumps and liquid nitrogen traps. At each decomposition temperature, about 20 experimental points of weight loss as a function of time were recorded.

The stoichiometry of the reaction was previously verified by TG, DTG and DTA analyses, in the temperature range 20–1000° C at a heating rate of 10° C min^{-1}. The resulting curves were compared with studies reported in the literature. The X-ray analyses were carried out for two hematite samples obtained at

0022–2461/89 $03.00 + .12 © *1989 Chapman and Hall Ltd.*

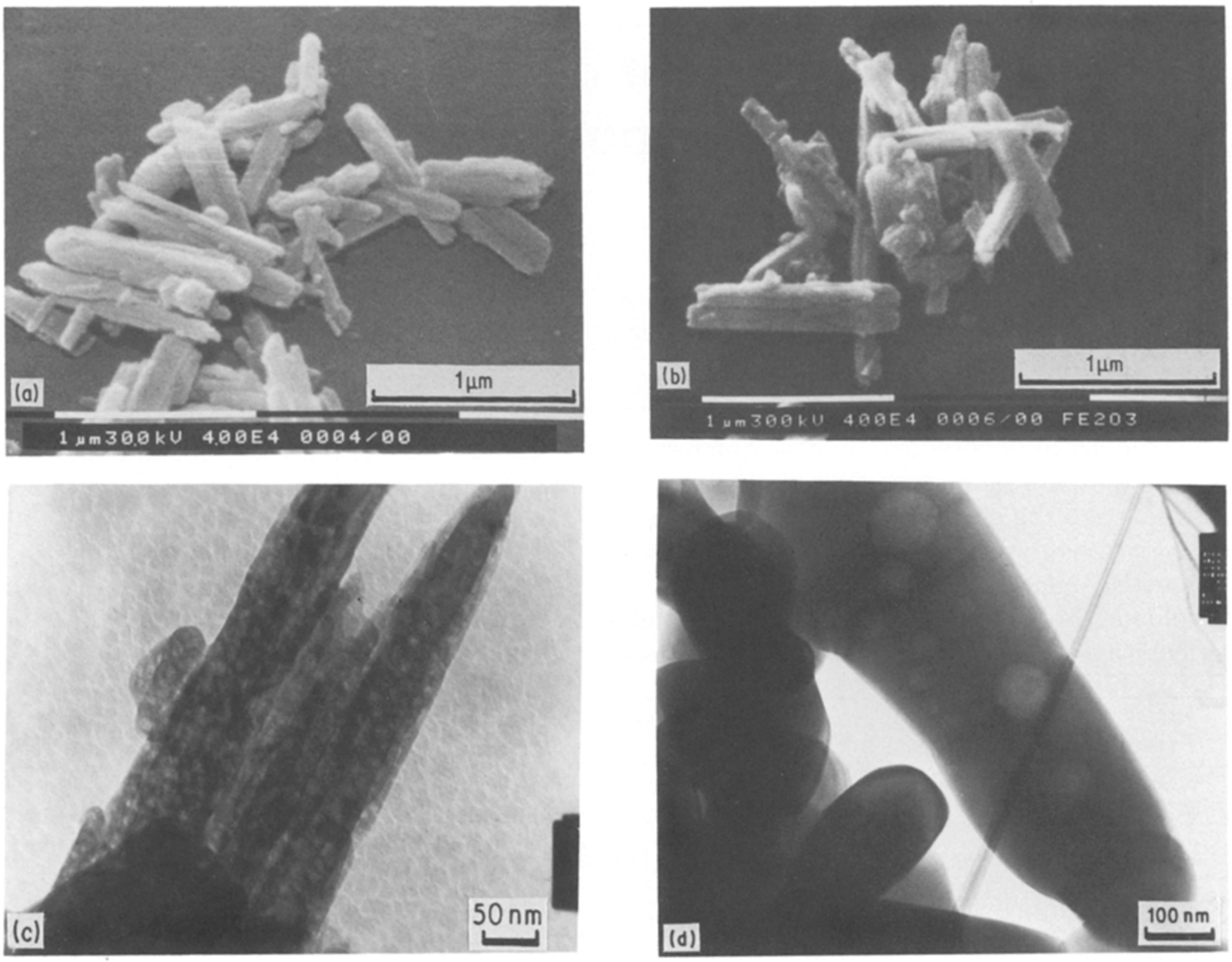

Figure 1 (a) α-goethite particles (SEM × 40 000). (b) α-hematite particles obtained at 225° C (SEM × 40 000). (c) Micropores in the α-hematite particles obtained at 225° C (TEM × 160 000). (d) Macropores in the α-hematite particles obtained at 1000° C (TEM × 108 000).

500 and 1000° C. The diffractograms were those of pure hematite, with sharper lines of diffraction for the sample obtained at 1000° C.

In separate experiments, about 1 g of goethite was completely decomposed, at temperatures of 175, 200, 225, 250 and 275° C, with the same procedure and experimental conditions previously described. The specific area of α-Fe_2O_3 was measured by the liquid nitrogen BET method. Transmission electron and scanning electron photographs were taken, employing a 300 kV energy TEM and a 30 kV energy SEM.

3. Results and discussion

Fig. 2 shows the function $\beta = (1 - X) \times 100$ as a function of time, where X is the conversion of goethite, experimentally determined.

For the interpretation of the data the shrinking core model for cylindrical particles [20] was utilized

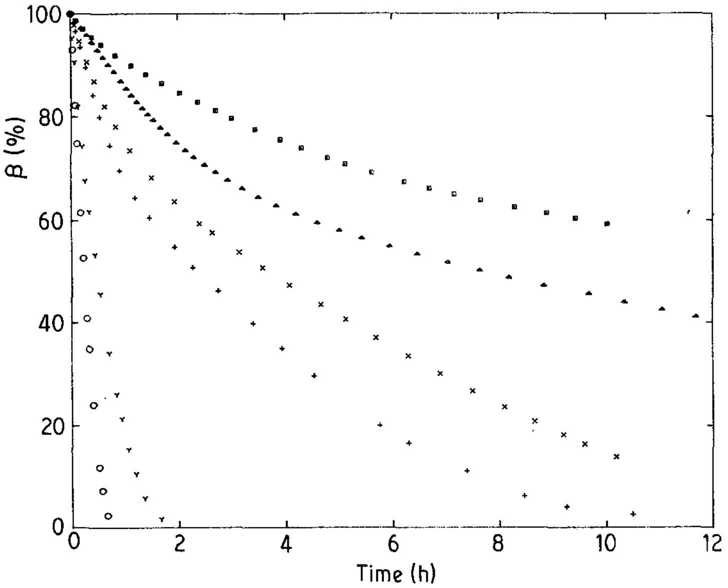

Figure 2 Decomposition curves of acicular α-geothitie at different experimental temperatures (■ 170° C ▲ 180° C, x 190° C, + 200° C Y 225° C, o 250° C).

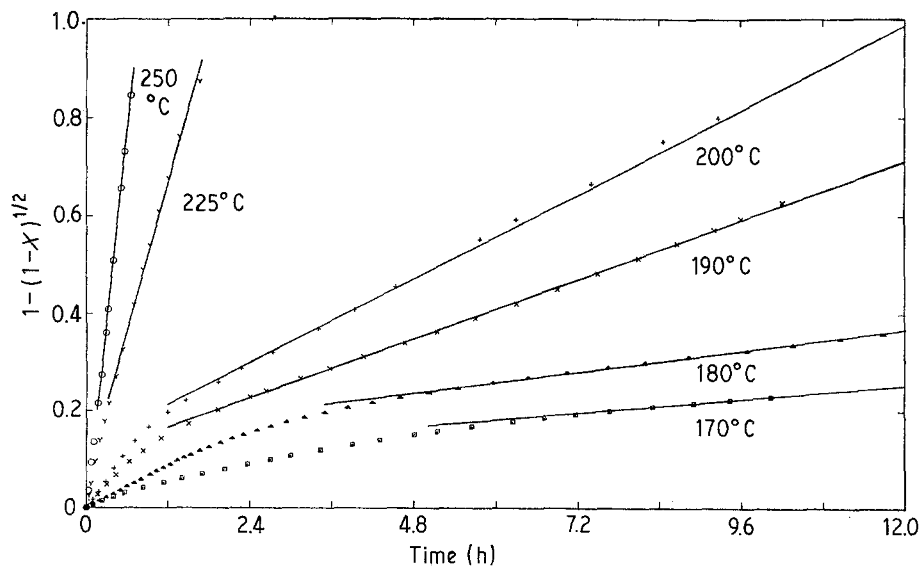

Figure 3 Plot of $[1 - (1 - X)^{1/2}]$ against time and relative straight lines obtained by least square treatment of the data.

assuming the rate determining step was the diffusion of the proton from the acceptor regions to the donor regions that will gradually transform into pores [4, 19]. This model is made explicit through the relation

$$1 - (1 - X)^{1/2} = \frac{KM}{\delta r_0} t \qquad (2)$$

In the above expression X again represents the conversion of the goethite, K is the kinetic constant of the process, δ the density of the goethite [21], M the molecular weight of the goethite and r_0 the average radius of the reacting particles, experimentally determined. The length of the particles was assumed to have no influence on the rate of decomposition.

An inspection of the curves reported in Fig. 3, where the function $[1 - (1 - X)^{1/2}]$ is plotted against time, shows a linear trend, after about 0.30 conversion. This behaviour was attributed to the presence of particles with dimension smaller than the average values calculated and employed in Equation 2.

In Table I are reported the slopes, S, and the intercepts, B, of the straight line obtained by least square treatment of the experimental data. At each temperature, the kinetic constant of the process, K, can be obtained, by the relation $S = KM/\delta r_0$. The K and $\ln K$ values are also reported in Table I. The activation energy of the transformation is related to the kinetic constant by the Arrhenius equation

$$\ln K = \ln A - E_a/RT \qquad (3)$$

The least square treatment of $\ln K$ against $1/T$ data yielded a value of the activation energy, $E_a = 119 \pm 9\,\mathrm{kJ\,mol^{-1}}$, at the average temperature of 210° C. The associated error takes into account the standard deviation from the mean and the error associated with the K values. The plot of $\ln K$ against $1/T$ is shown in Fig. 4.

3.1. Specific area and pore structure

The results of specific area measurements, obtained by nitrogen adsorption on the surface of hematite at the temperature of liquid nitrogen, are reported in Table II are plotted in Fig. 5. It can be seen that the maximum specific area of hematite corresponds to a decomposition temperature of about 225° C.

This result can be explained through a combined process of pore formation, due to the evaporation of H_2O from the structure, and rearrangement of the high stressed surface and structure. Both these mechanisms are enhanced by increasing the temperature, but with opposite effects on the specific area. At about 225° C the best balance is obtained. Visual observation by SEM of goethite (Fig. 1a) and hematite (Fig. 1b) did not show any significant change in the morphology of the particles. Observations carried out at × 100 000 magnification did not reveal the presence of pores in the surface either. TEM observations of the hematite obtained at 225° C, showed the existence of micropores, of about 2.5 nm average diameter, aligned along the main axis of the particle (Fig. 1c). Fig. 1d is a TEM photograph relating to the hematite obtained at 1000° C, and shows the presence of spherical micropores of about 50 nm average diameter located in the centre of the particle.

TABLE I Slopes (S) and intercepts (B) of the straight lines describing the decomposition of α-goethite at the experimental temperature T, and relative kinetic constant k

T (°C)	$(1/T)^{10^{-3}}$ ($\mathrm{K^{-1}}$)	S ($\times 10^2$)	B ($\times 10^2$)	$k \times 10^{-5}$ ($\mathrm{mol\,m^{-2}\,h^{-1}}$)	$\ln k$
170	2.257	1.21 ± 0.03	10.92 ± 0.23	5.795	−9.756
180	2.207	1.82 ± 0.03	14.96 ± 0.28	8.731	−9.346
190	2.159	5.07 ± 0.27	10.52 ± 0.18	24.359	−8.320
200	2.113	7.16 ± 1.54	12.76 ± 0.92	34.395	−7.975
225	2.007	50.80 ± 1.04	5.79 ± 1.03	244.429	−6.014
250	1.911	132.29 ± 0.53	−2.07 ± 0.22	635.191	−5.059

The associated error is the standard deviation from the mean.

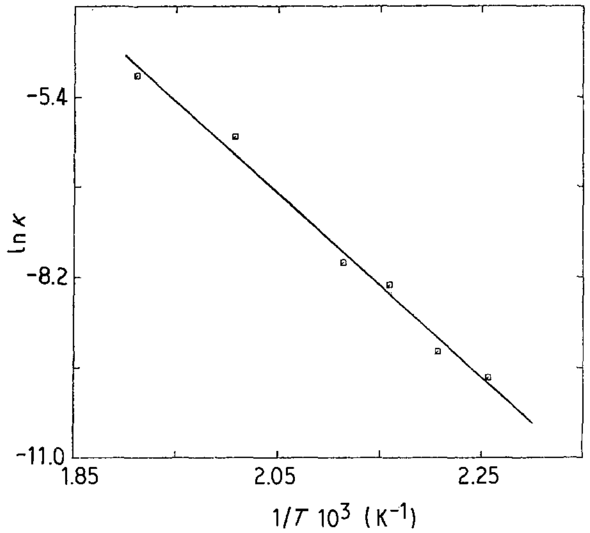

Figure 4 Temperature dependence of the kinetic constant k and interpolation straight line $E_a = 119 \pm 9\,\mathrm{kJ\,mol^{-1}}$.

4. Conclusion

The two possible rate determining steps of the decomposition of goethite into hematite are the diffusion of the protons from the acceptor regions to the donor regions and the diffusion of the water molecules through the pores. These two mechanisms correspond to different mathematical relations in the shrinking core model for cylindrical particles [20].

Our experimental data fitted well with the mathematical approach that considers the diffusion of the proton in the structure as the controlling step.

The energy of activation value, $E_a = 119 \pm 9\,\mathrm{kJ\,mol^{-1}}$ is in agreement with previous determinations [4] obtained in a temperature range higher than the one considered here.

From the observation of α-FeOOH and Fe_2O_3 particles by SEM and TEM techniques it can be seen that the micropores have essentially a slit-shape with dimensions ranging from 1 to 5 nm and are aligned along the main axis of the particles.

It is also evident that the formation of pores is mainly a bulk phenomenon, since no apparent difference in morphology was noticed by observing the surfaces of goethite and hematite at × 100 000 magnification. These observations support the results obtained in previous investigations [8]. If the decomposition temperature is increased to 1000° C the pores evolve in spherical macropores, ranging from 15 to 100 nm diameter, and are positioned in the centre of the particle. This macroporosity can be ascribed to a structural rearrangement and coalescence of the micropores induced by the temperature. The morphology of hematite appears sensibly modified due to surface mobility.

TABLE II Specific area of α-hematite samples, by BET method, obtained at different decomposition temperatures

Decomposition temperature (° C)	S_{BET} ($m^2\,g^{-1}$)
175	102.1 ± 5.0
200	105.7 ± 6.5
225	118.4 ± 5.5
250	116.6 ± 7.4
275	104.7 ± 5.2

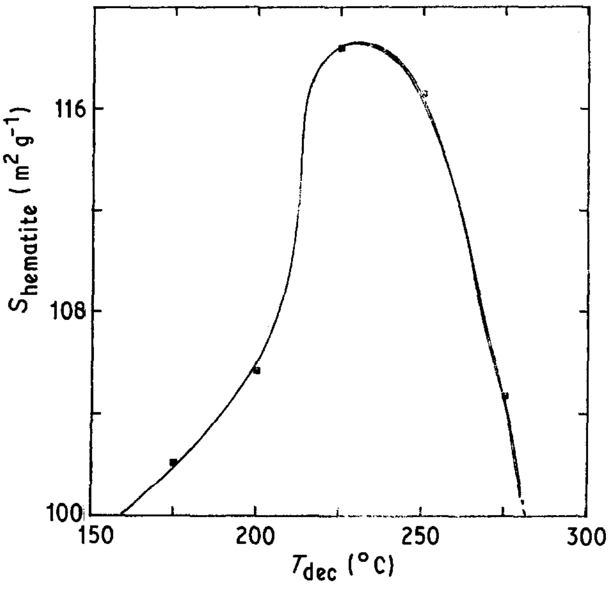

Figure 5 Behaviour of the specific area, S_{BET}, of α-hematite as function of the decomposition temperature of α-goethite.

Acknowledgements

The authors are sincerely grateful to Mrs Luisa Corona and Mrs Maria Giammatteo for the collaboration in using the TEM and SEM techniques.

References

1. J. ERVIN, *Acta Crystall.* **5** (1952) 103.
2. S. J. GREEG and K. J. HILL, *J. Appl. Chem.* **1** (1953) 3945.
3. M. H. FRANCOMBE and H. P. ROOKSBY, *Clay Miner. Bull.* **4** (1959) 1.
4. J. LIMA DE FARIA, *Z. Krist.* **119** (1963) 176.
5. J. LIMA DE FARIA and P. GAY, *Miner. Mag.* **33** (1962) 37.
6. T. YAMAGUCHI and T. TAKAHASHI, *J. Amer. Ceram. Soc.* **65** (1982) C83.
7. D. BERUTO, *Mater. Chem. Phys.* **8** (1983) 233.
8. S. HIROKAWA, T. NAITO and T. YAMAGUCHI, *J. Colloid Interface Sci.* **112** (1986) 268.
9. F. WATARI, J. VAN LANDUYT, P. DELAVIGNETTE and S. AMELINCKX, *J. Solid State Chem.* **29** (1979) 137.
10. J. MAEDA, M. IGARASHI, A. TERADA and F. YOSHIMURA, *Jpn J. Appl. Phys.* **13** (1974) 381.
11. W. VAN OOSTERHOUT, *Acta Crystallogr.* **13** (1960) 932.
12. N. YAMAMOTO, T. SHINJO, M. KIJAMA, Y. BANDO and T. TAKODA, *J. Phys. Soc. Jpn* **25** (1968) 1267.
13. F. WATARI, P. DELAVIGNETTE, J. VAN LANDUYT and S. AMELINCKX, *J. Solid State Chem.* **48** (1983) 49.
14. H. NAONO and R. FUJIWARA, *J. Colloid Interface Sci.* **96** (1976) 162.
15. D. T. PRICHARD and E. C. ORMEROD, *Clay Miner.* **11** (1976) 327.
16. T. ISHIKAWA and K. INOUYE, *Bull. Chem. Soc. Jpn* **45** (1972) 2350.
17. T. ASAI, S. NOBUOKA and K. ANDO, *Nippon Kagaku Kaishi*, (1978) 654.
18. L. VOLPE and M. BOUDART, *Catal. Rev. Sci. Eng.* **27** (1985) 515.
19. M. C. BALL and H. F. TAYLOR, *Miner. Mag.* **32** (1961) 754–766.
20. O. LEVENSPIEL, "Ingegneria delle reazioni chimiche" (Department of Chemical Engineering, Oregon State University, Ed. Ambrosiana Milana 1978).
21. R. A. ROBIE, B. S. HEMINGWAY and J. R. FISHER, *US Geol. Survey Bull.* **1452** (1979).

Received 25 January
and accepted 10 June 1988